Title	Finite Element Formulation of the Nagtegaal-Rice Functional Using Constant Strain Triangles
Author(s)	MAEKAWA, katsuhiro / H.C.CHILDS, thomas
Citation	茨城大学工学部研究集報(39): 53-66
Issue Date	1991-12
URL	http://hdl.handle.net/10109/7389
Rights	

Finite Element Formulation of the Nagtegaal-Rice Functional Using Constant Strain Triangles

Katsuhiro MAEKAWA* and Thomas H.C.CHILDS**

(Received August 31, 1991)

Abstract —The finite element formulations based on the Nagtegaal-Rice functional for nearly incompressible deformation have been developed using a quadrilateral element which consists of a pair of constant strain triangles. The replacement of a varying hydrostatic component of strain rate in each triangle by the average for the pair could reduce overconstraint. Using such a constant dilatation quadrilateral element, the so-called updated Lagrangian approach is employed for the implementation. For plane strain finite deformation plasticity, several types of finite element are examined and their corresponding computational efficiency and accuracy are compared by means of examples of pure bending and uniaxial tension. The formulations developed in this paper are proved to be free of overconstraint and show reasonable computational efficiency.

NOMENCLATURE

a_0	half width of bar	$\{T_i\}$	surface traction
$[B]$	nodal velocity-strain rate matrix	t	time
$[D]$	elastic-plastic matrix	$\{\dot{u}\}$	nodal velocity
$[D_G]$	geometric nonlinear matrix	u^*	prescribed displacement
E	Young's modulus	V	volume
e_{ij}	Lagrange strain	w	thickness of element
$\dot{e}^m$	hydrostatic part of strain rate	$\{x\}$	Cartesian coordinates
$\{F\}$	nodal force	$[\ ]$	matrix
G	shear modulus	$\{\ \}$	vector
H'	work hardening rate	α^*	elastic-plastic parameter
h	thickness of beam	Δ	area of triangle
I	functional	Δt	time increment
ℓ_0	half length of bar	δ	virtual quantity
M	moment	δ_{ij}	Kronecker delta
M_{limit}	limit bending moment	$\bar{\varepsilon}^p$	equivalent plastic strain
N_i	shape function relevant to node i	ζ	amplitude
S	surface area	κ	bulk modulus
s_{ij}	Lagrange stress	ν	Poisson's ratio

* Department of Mechanical Engineering, Faculty of Engineering, Ibaraki University, Hitachi 316, Japan

** Department of Mechanical Engineering, University of Leeds, Leeds LS2 9JT, UK

$\bar{\sigma}$	equivalent stress	avg	average
σ_{ij}	Euler stress	B	element B
σ_y	yield stress	mod	modified quantity
$\dot{\phi}$	dilational strain rate	T	transposed matrix or vector
χ	curvature	t	time at t
$\dot{\omega}$	rate of rotation	$t+\Delta t$	time at $t+\Delta t$
		0	initial value
Superscripts and subscripts		$'$	deviatoric component
A	element A	$\cdot$	material derivative
		$*$	Jaumann derivative

1. INTRODUCTION

The three-node constant strain triangular element [1] has successfully been employed for elastic-plastic analysis with small scale yielding as well as elastic analysis. In the fully plastic range, however, it has been pointed out that the response of the element is too stiff to simulate the real mode of deformation. This is due to the requirement of vanishing volumetric strain increment in the constitutive equations, although with strain hardening part of the strain increment is elastic. A special arrangement of a quadrilateral element which consists of four constant strain triangles obtained by connecting its diagonals was proved to be free of overconstraint for plane strain problems [2]. This model, however, brings an inevitable increase in the number of nodes and elements, resulting in poor efficiency of the computation. Another approach is to modify variational principles so as to be applied to the problems with incompressible deformation [2, 3].

Based on the Nagtegaal-Rice functional [2], the present paper proposes a finite element formulation using a quadrilateral element which consists of two constant strain triangles. Treating the triangles as a pair not only breaks through the overconstraint problem but also keeps the number of nodes unchanged, leading to a saving of CPU time. The Nagtegaal-Rice functional and its modification to a pair of finite elements are described in the following section. Then, the formulation with the modified functional is implemented for a pair of triangular elements, and a couple of examples such as pure bending and plane strain uniaxial tension are shown to discuss the nature of the solutions in comparison with the conventional finite element method.

2. THE NAGTEGAAL - RICE FUNCTIONAL AND ITS MODIFICATION

Incremental virtual work in a continuum [4] gives

$$\int_S \dot{T}_i \dot{u}_i \, dS = \int_V \dot{s}_{ij} \dot{e}_{ij} \, dV \tag{1}$$

where a body force term is neglected. The volume work rate in the right-hand side may be split into a deviatoric part $\dot{s}'_{ij} \dot{e}'_{ij}$ and a hydrostatic part $\kappa (\dot{e}_{kk})^2$ where κ is the bulk modulus, giving

$$\int_S \dot{T}_i \dot{u}_i \, dS = \int_V \dot{s}'_{ij} \dot{e}'_{ij} \, dV + \kappa \int_V (\dot{e}_{kk})^2 \, dV \tag{2}$$

As the term $\int_V \dot{s}'_{ij} \dot{e}'_{ij} \, dV$ is positive during the deformation,

$$\int_S \dot{T}_i \dot{u}_i \, dS > \kappa \int_V (\dot{e}_{kk})^2 \, dV \tag{3}$$

If $\dot{T}_i$ approaches zero, as it does in problems with a limit load, then $\dot{e}_{kk}$ approaches zero as well. This relation holds on an elastic level as well as the more obvious plastic level.

Nagtegaal et al. [2] then show that in a finite element approximation $\dot{e}_{kk} = 0$ can lead to problems : for example, for a three-node triangular element in plane strain, strain rates are constant within an element. If one component of $\dot{e}_{kk}$, say $\dot{e}_{11}$ is specified on one boundary of an element, then $\dot{e}_{kk} = 0$ specifies the other component. These components, being constant within the element, then lead to specified components in neighbouring elements and so on. This causes an over-severe restraint on element deformation. The combination of four three-noded triangles as shown in Fig. 1 (a), where the triangular element boundaries form a quadrilateral element and its diagonals, only successfully makes the arrangement suitable for analysis in the fully plastic range.

Nagtegaal et al. [2] suggest a way out: modify the definition of strain rate in an element as far as its hydrostatic component is concerned: for any element instead of defining strain rate at any point A as $\dot{e}_A = \dot{e}'_A + \dot{e}^m_A$, where the superscript m means hydrostatic part, replace it by $\dot{e}_A = \dot{e}'_A + (\dot{e}^m)_{avg}$, i.e. replace the varying hydrostatic part by the average for the element. They also demonstrate how this reduces overconstraint, and develop the argument for a four-node quadrilateral element.

The four-node quadrilateral element requires Gauss's numerial integration which is disadvantageous from the viewpoint of computational time. On the other hand, the three-node element interpolated by a linear function has no need for integration procedures. Consequently, it seems most desirable that the Nagtegaal-Rice functional be formulated using the constant strain triangle.

The functional presented by Nagtegaal et al. [2] is

$$I = \int_V \left(\frac{1}{2} \dot{s}'_{ij} \dot{e}'_{ij} + \kappa \dot{\phi} \dot{u}_{k,k} - \frac{1}{2} \kappa \dot{\phi}^2 \right) dV - \int_S \dot{T}_i \dot{u}_i \, dS \tag{4}$$

where the first term in the right side denotes deviatoric work rate and the second and third ones are related to dilatation work rate, but $\dot{\phi}$ is constant over the volume V. Now consider the

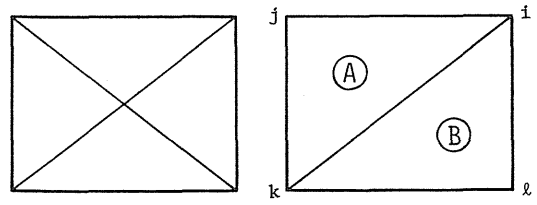

(a) Crossed triangles (b) Constant dilatation triangles

Fig. 1 Approximation of a quadrilateral by triangles

functional I below evaluated over the pair of elements A and B, where in the case of Fig. 1 (b) A+B makes a quadrilateral element. Then,

$$I = \int_{V_A} \left(\frac{1}{2} \dot{s}'_{ij} \dot{e}'_{ij} + \kappa \dot{\phi} \dot{u}^{A}_{k,k} - \frac{1}{2} \kappa \dot{\phi}^2 \right) dV$$

$$+ \int_{V_B} \left(\frac{1}{2} \dot{s}'_{ij} \dot{e}'_{ij} + \kappa \dot{\phi} \dot{u}^{B}_{k,k} - \frac{1}{2} \kappa \dot{\phi}^2 \right) dV - \int_{S_A + S_B} \dot{T}_i \dot{u}_i \, dS \qquad (5)$$

$\dot{\phi}$ is an additional variable, i.e. degree of freedom, which is defined by an interpretation from $\partial I / \partial \dot{\phi} = 0$:

$$\frac{\partial I}{\partial \dot{\phi}} = \int_{V_A} \left(\kappa \dot{u}^{A}_{k,k} - \kappa \dot{\phi} \right) dV + \int_{V_B} \left(\kappa \dot{u}^{B}_{k,k} - \kappa \dot{\phi} \right) dV = 0 \qquad (6)$$

Hence,

$$\dot{\phi} = \frac{\int_{V_A} \dot{u}^{A}_{k,k} \, dV + \int_{V_B} \dot{u}^{B}_{k,k} \, dV}{\int_{V_A} dV + \int_{V_B} dV} \qquad (7)$$

Equation (7) means that $\dot{\phi}$ is the average of dilatation over the elements A and B. Equation (7) enables Eq. (5) to be simplified as

$$I = \int_{V_A} \left(\frac{1}{2} \dot{s}'_{ij} \dot{e}'_{ij} + \frac{1}{2} \kappa \dot{\phi}^2 \right) dV$$

$$+ \int_{V_B} \left(\frac{1}{2} \dot{s}'_{ij} \dot{e}'_{ij} + \frac{1}{2} \kappa \dot{\phi}^2 \right) dV - \int_{S_A + S_B} \dot{T}_i \dot{u}_i \, dS \qquad (8)$$

If one defines modified stresses and strains as

$$\left.\begin{aligned} \dot{s}^{mod}_{ij} &= \dot{s}'_{ij} + \kappa \dot{\phi} \delta_{ij} \\ \dot{e}^{mod}_{ij} &= \dot{e}'_{ij} + \frac{1}{3} \dot{\phi} \delta_{ij} \end{aligned}\right\} \qquad (9)$$

where δ_{ij} is the Kronecker delta, one obtains

$$\frac{1}{2} \dot{s}^{mod}_{ij} \dot{e}^{mod}_{ij} = \frac{1}{2} \dot{s}'_{ij} \dot{e}'_{ij} + \frac{1}{2} \kappa \dot{\phi}^2$$

Consequently, the functional (8) becomes

$$I = \int_{V_A} \frac{1}{2} \dot{s}_{ij}^{mod} \dot{e}_{ij}^{mod} \, dV + \int_{V_B} \frac{1}{2} \dot{s}_{ij}^{mod} \dot{e}_{ij}^{mod} \, dV - \int_{S_A + S_B} \dot{T}_i \dot{u}_i \, dS \tag{10}$$

and this is the same form as the conventional variational one [4]. By taking the first variation in $\dot{u}_i$ and setting it to zero, one finds

$$\delta I = \int_{V_A} \dot{s}_{ij}^{mod} \delta \dot{e}_{ij}^{mod} \, dV + \int_{V_A} \dot{s}_{ij}^{mod} \delta \dot{e}_{ij}^{mod} \, dV - \int_{S_A + S_B} \dot{T}_i \delta \dot{u}_i \, dS = 0 \tag{11}$$

Equation (11) may yield a solution with respect to $\dot{u}_i$.

We consider the motion of a body in a stationary Cartesian, or fixed linear orthogonal coordinate system, as shown in Fig. 2. As for definitions of stress and strain to deal with large deformation and/or geometric nonlinear problems, several measures have been proposed [5]. On the basis of the updated Lagrangian approach, we use the Jaumann derivative of Euler stress $\{\dot{\sigma}^*\}$ in conjunction with the modified velocity strain $\{\dot{e}^{mod}\}$ and the rate of modified Lagrange stress $\{\dot{s}^{mod}\}$ where the following relationship between $\{\dot{\sigma}^*\}$ and $\{\dot{s}^{mod}\}$ holds

$$\{\dot{\sigma}^*\} = \{\dot{s}^{mod}\} - [D_G] \{\dot{e}^{mod}\} \tag{12}$$

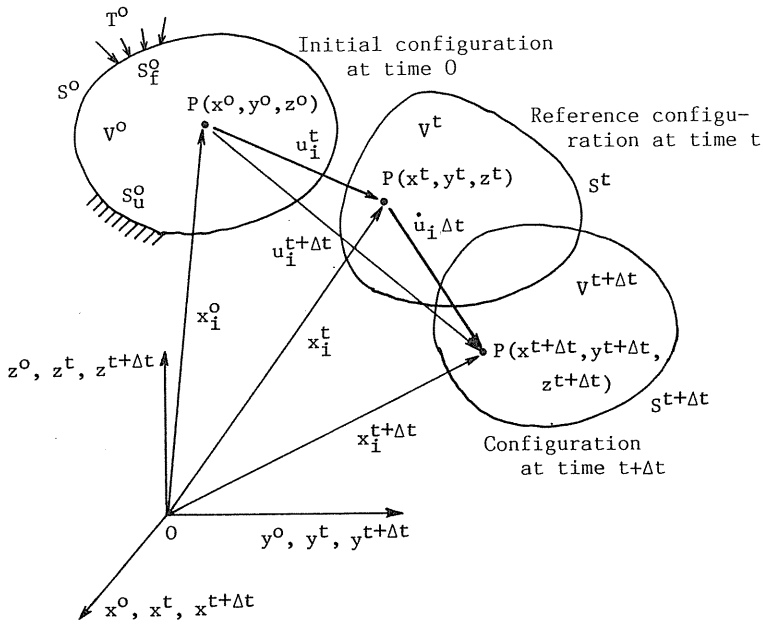

Fig. 2 Motion of body in stationary Cartesian coordinates

$[D_G]$ is the geometric nonlinear term. And we postulate a constitutive equation as

$$\{\overset{*}{\dot{\sigma}}\} = [D] \{\dot{e}^{\mathrm{mod}}\} \tag{13}$$

where $[D]$ is the elastic stress-strain matrix for elastic deformation or the elastic-plastic stress-strain matrix for plastic deformation. Forms of $[D_G]$ and $[D]$ will be specified in the next section.

Accoring to the standard procedure of finite element formulation, the virtual strain rate $\{\delta \dot{e}^{\mathrm{mod}}\}$ may have a relationship with the virtual nodal velocity $\{\delta \dot{u}\}$ as

$$\{\delta \dot{e}^{\mathrm{mod}}\} = [B^{\mathrm{mod}}] \{\delta \dot{u}\} \tag{14}$$

where $[B^{\mathrm{mod}}]$ is the velocity-strain rate matrix. The substitution of Eqs. (12) − (14) into Eq. (11) yields the elemental stiffness equation in matrix form as

$$\left(\int_{V_A} [B^{\mathrm{mod}}]^{\mathrm{T}} ([D] + [D_G]) [B^{\mathrm{mod}}] \, dV + \int_{V_B} [B^{\mathrm{mod}}]^{\mathrm{T}} ([D] + [D_G]) [B^{\mathrm{mod}}] \, dV\right) \{\dot{u}\} = \{\dot{F}\}_A + \{\dot{F}\}_B \tag{15}$$

where $\{\dot{F}\}_A$ and $\{\dot{F}\}_B$ are the specified nodal force rate over the elements A and B, respectively.

3. IMPLEMENTATION USING A PAIR OF TRIANGULAR ELEMENTS

We confine the implementation to plane strain problems using a pair of triangular elements. According to the standard procedures of the finite element method [1], velocity within the element A of Fig. 1 (b), $\{\dot{u}\}_A = \{\dot{u}\ \dot{v}\}_A^{\mathrm{T}}$, is given by a linear interpolaion using nodal velocities $\{\dot{u}\} = \{\dot{u}_i\ \dot{v}_i\ \dot{u}_j\ \dot{v}_j\ \dot{u}_k\ \dot{v}_k\}^{\mathrm{T}}$ as

$$\{\dot{u}\}_A = \left[[I]\ N_i \quad [I]\ N_j \quad [I]\ N_k\right] \{\dot{u}\} \tag{16}$$

where $[I]$ is unit matrix of order 2×2, N_i is given by

$$\left.\begin{aligned} N_i &= (a_i + b_i x + c_i y) \ / \ 2\Delta_A \\ a_i &= x_j y_k - x_k y_j \\ b_i &= y_j - y_k \\ c_i &= x_k - x_j \end{aligned}\right\} \tag{17}$$

with the other coefficients obtained by a cyclic permutation of subscripts in the order i, j and k, and

$$\Delta_A = \frac{1}{2} \det \begin{vmatrix} 1 & x_i & y_i \\ 1 & x_j & y_j \\ 1 & x_k & y_k \end{vmatrix} \tag{18}$$

which is the area of the triangle A.

Since the modified velocity strains of Eq. (9) within the element A can be described as

$$\{\dot{e}^{mod}\}_A = \begin{Bmatrix} \dot{e}_x^{mod} \\ \dot{e}_y^{mod} \\ \dot{e}_z^{mod} \\ \dot{e}_{xy} \\ \dot{e}_{yx} \end{Bmatrix}_A = \begin{Bmatrix} \frac{2}{3}\dot{e}_x - \frac{1}{3}\dot{e}_y \\ -\frac{1}{3}\dot{e}_x + \frac{2}{3}\dot{e}_y \\ -\frac{1}{3}(\dot{e}_x + \dot{e}_y) \\ \dot{e}_{xy} \\ \dot{e}_{yx} \end{Bmatrix}_A + \frac{\dot{\phi}}{3}\begin{Bmatrix} 1 \\ 1 \\ 1 \\ 0 \\ 0 \end{Bmatrix} \tag{19}$$

where

$$\dot{\phi} = \frac{(\dot{e}_x + \dot{e}_y)_A \Delta_A + (\dot{e}_x + \dot{e}_y)_B \Delta_B}{\Delta_A + \Delta_B} \tag{20}$$

and $\dot{e}_{ij} = \partial \dot{u}_j / \partial x_i$ as usual, the similar expresion of Eq. (14) may be obtained:

$$\{\dot{e}^{mod}\}_A = [B^{mod}]_A \{\dot{u}\} \tag{21}$$

where

$$[B^{mod}]_A = \frac{1}{6\Delta_A}\begin{bmatrix} 2b_i & -c_i & 2b_j & -c_j & 2b_k & -c_k & 0 & 0 \\ -b_i & 2c_i & -b_j & 2c_j & -b_k & 2c_k & 0 & 0 \\ -b_i & -c_i & -b_j & -c_j & -b_k & -c_k & 0 & 0 \\ 3c_i & 0 & 3c_j & 0 & 3c_k & 0 & 0 & 0 \\ 0 & 3b_i & 0 & 3b_j & 0 & 3b_k & 0 & 0 \end{bmatrix}_A$$

$$+ \frac{1}{6(\Delta_A + \Delta_B)}\begin{bmatrix} b_i^A + b_i^B & c_i^A + c_i^B & b_j^A & c_j^A & b_k^A + b_k^B & c_k^A + c_k^B & b_\ell^B & c_\ell^B \\ b_i^A + b_i^B & c_i^A + c_i^B & b_j^A & c_j^A & b_k^A + b_k^B & c_k^A + c_k^B & b_\ell^B & c_\ell^B \\ b_i^A + b_i^B & c_i^A + c_i^B & b_j^A & c_j^A & b_k^A + b_k^B & c_k^A + c_k^B & b_\ell^B & c_\ell^B \\ 0 & 0 & 0 & 0 & 0 & 0 & 0 & 0 \\ 0 & 0 & 0 & 0 & 0 & 0 & 0 & 0 \end{bmatrix} \tag{22}$$

We have already decided to use the constitutive equation of Eq. (13) which connects the Jaumann derivatives of Euler stress $\{\overset{*}{\sigma}\} = \{\overset{*}{\sigma}_x \overset{*}{\sigma}_y \overset{*}{\sigma}_z \overset{*}{\tau}_{xy} \overset{*}{\tau}_{yx}\}^T$ with the modified velocity strain $\{\dot{e}^{mod}\}$. If we postulate an isotropic work hardening material which obeys the Mises yield criterion and the Prandtl-Reuss flow rule, the stress-strain matrix $[D]$ is given by

$$[D] = \frac{E}{1+\nu}\begin{bmatrix} \frac{1-\nu}{1-2\nu} & \frac{\nu}{1-2\nu} & \frac{\nu}{1-2\nu} & 0 & 0 \\ & \frac{1-\nu}{1-2\nu} & \frac{\nu}{1-2\nu} & 0 & 0 \\ & & \frac{1-\nu}{1-2\nu} & 0 & 0 \\ & & & \frac{1}{2} & \frac{1}{2} \\ & \text{sym} & & & \frac{1}{2} \end{bmatrix}$$

$$-\alpha^* \frac{9G^2}{\bar{\sigma}^2(H'+3G)} \begin{bmatrix} \sigma'_x{}^2 & \sigma'_y\sigma'_x & \sigma'_z\sigma'_x & \tau_{xy}\sigma'_x & \tau_{yx}\sigma'_x \\ \sigma'_x\sigma'_y & \sigma'_y{}^2 & \sigma'_z\sigma'_y & \tau_{xy}\sigma'_y & \tau_{yx}\sigma'_y \\ \sigma'_x\sigma'_z & \sigma'_y\sigma'_z & \sigma'_z{}^2 & \tau_{xy}\sigma'_z & \tau_{yx}\sigma'_z \\ \sigma'_x\tau_{xy} & \sigma'_y\tau_{xy} & \sigma'_z\tau_{xy} & \tau_{xy}{}^2 & \tau_{yx}\tau_{xy} \\ \sigma'_x\tau_{yx} & \sigma'_y\tau_{yx} & \sigma'_z\tau_{yx} & \tau_{xy}\tau_{yx} & \tau_{yx}{}^2 \end{bmatrix} \tag{23}$$

where $\alpha^* = 0$ for elastic deformation and $\alpha^* = 1$ for the plastic state. The geometric nonlinear matrix $[D_G]$ in Eq. (12) has the following form:

$$[D_G] = \begin{bmatrix} 0 & \sigma_x & \sigma_x & -\tau_{xy} & 0 \\ \sigma_y & 0 & \sigma_y & 0 & -\tau_{xy} \\ \sigma_z & \sigma_z & 0 & 0 & 0 \\ 0 & \tau_{xy} & \tau_{xy} & \frac{1}{2}(\sigma_x-\sigma_y) & -\frac{1}{2}(\sigma_x+\sigma_y) \\ \tau_{xy} & 0 & \tau_{xy} & -\frac{1}{2}(\sigma_x+\sigma_y) & \frac{1}{2}(\sigma_x-\sigma_y) \end{bmatrix} \tag{24}$$

Consequently, using the matrices $[B^{mod}]$, $[D]$ and $[D_G]$ of Eqs. (22), (23) and (24), respectively, the elemental siffness equation (15) for a pair of triangular elements A and B may be obtaind as

$$w\left[\left([B^{mod}]^T\left([D]+[D_G]\right)[B^{mod}]\,\Delta\right)_A + \left([B^{mod}]^T\left([D]+[D_G]\right)[B^{mod}]\,\Delta\right)_B\right]\{\dot{u}\} = \{\dot{F}\}_A + \{\dot{F}\}_B \tag{25}$$

where w is the thickness of the elements.

We finally obtain the global stiffness equations by summing up Eq. (25) over all the pairs. Solving them with respect to the unknown nodal velocity $\{\dot{u}\}$ under given boundary conditions, and then substituting $\{\dot{u}\}$ into Eq. (21), the modified velocity strains $\{\dot{e}^{mod}\}$ within an individual element are obtained. Then substituting $\{\dot{e}^{mod}\}$ into Eq. (13), we obtain the Jaumann rates of Euler stress $\{\overset{*}{\sigma}\}$ within an element. However, $\{\overset{*}{\sigma}\}$ is the stress observed in a rectangular coordinate system rotating with the body. It is not influenced by a rigid body rotation of the material. We ought to calculate the Euler stress rate $\{\dot{\sigma}\}$ within an element, which is defined in the fixed Cartesian coordinate system. The two stresses have the following relationship [6]:

$$[\overset{*}{\sigma}] = [\dot{\sigma}] - [\dot{\omega}]^{T}[\sigma] - [\sigma][\dot{\omega}] \tag{26}$$

or

$$\{\dot{\sigma}\} = \begin{Bmatrix} \dot{\sigma}_x \\ \dot{\sigma}_y \\ \dot{\sigma}_z \\ \dot{\tau}_{xy} \end{Bmatrix} = \begin{Bmatrix} \overset{*}{\sigma}_x \\ \overset{*}{\sigma}_y \\ \overset{*}{\sigma}_z \\ \overset{*}{\tau}_{xy} \end{Bmatrix} + \begin{Bmatrix} -2\tau_{xy} \\ 2\tau_{xy} \\ 0 \\ \sigma_x - \sigma_y \end{Bmatrix} \dot{\omega} \tag{26}'$$

where $\dot{\omega}$ is the angular velocity, being defined by

$$\dot{\omega} = \frac{1}{2}\left(\frac{\partial \dot{v}}{\partial x} - \frac{\partial \dot{u}}{\partial y}\right) \tag{27}$$

Using Eq. (16), Eq. (27) can be written as

$$\dot{\omega} = \frac{1}{4\Delta_A}\left(-c_i\dot{u}_i + b_i\dot{v}_i - c_j\dot{u}_j + b_j\dot{v}_j - c_k\dot{u}_k + b_k\dot{v}_k\right) \tag{28}$$

Multiplying these quantities by the time increment Δt and adding them to those values which have been obtained in the previous stage of deformation, i.e. at time t of Fig. 2, we may obtain the updated values of the coordinate $\{x\}$, strain $\{e^{mod}\}$, stress $\{\sigma\}$ and nodal force $\{F\}$ at time $t+\Delta t$:

$$\left.\begin{aligned} \{x\}^{t+\Delta t} &= \{x\}^{t} + \{\dot{u}\}\,\Delta t \\ \{e^{mod}\}^{t+\Delta t} &= \{e^{mod}\}^{t} + \{\dot{e}^{mod}\}\,\Delta t \\ \{\sigma\}^{t+\Delta t} &= \{\sigma\}^{t} + \{\dot{\sigma}\}\,\Delta t \\ \{F\}^{t+\Delta t} &= \{F\}^{t} + \{\dot{F}\}\,\Delta t \end{aligned}\right\} \tag{29}$$

Repeating such an incremental calculation, we can perform general elastic-plastic analysis with large displacements and rotations and large strains.

4. NUMERICAL EXAMPLES

4.1 Pure Bending of an Elastic-Plastic Beam

We consider the simple example of a beam, in order to compare the accuracy and the corresponding computational efficiency of the various considered elements: regular constant strain triangle (CST), 4-crossed constant strain triangles (4 CST), 4-noded isoparametric (4 ISO) and the averaged dilatation constant strain triangles (CDT). It is assumed that plane sections perpendicular to the beam's axis remain plane during the deformation, and a slice of unit thickness subjected to the prescribed displacement, u^*, as shown in Fig. 3 (d), is considered. For

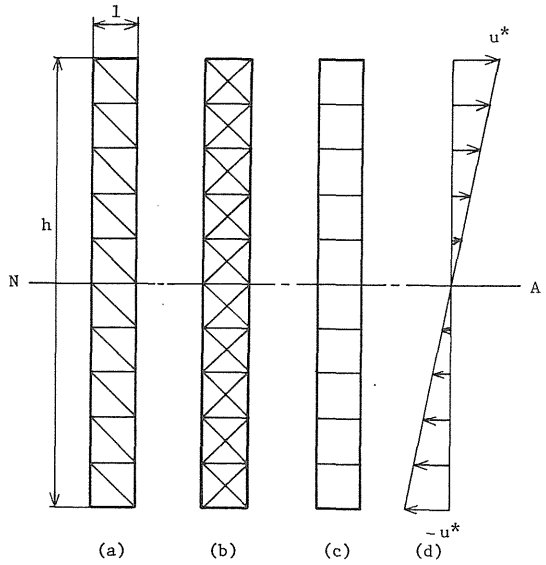

Fig. 3 Finite element systems for pure bending

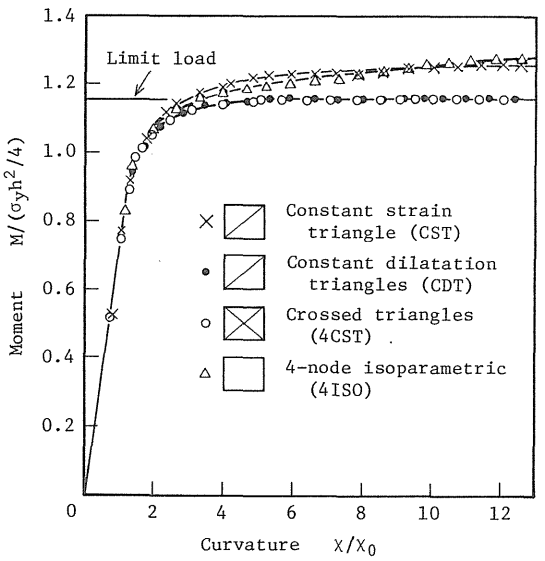

Fig. 4 Moment-curvature curves for various types of finite element

CST and CDT elements the finite element mesh shown in Fig. 3 (a), for 4 CST the finite element 3 (b), and for 4 ISO the finite element 3 (c) are, respectively, used. A unit increment of curvature is 0.00001, and the incremental displacement is applied until the moment-curvature curve attains a constant value. The beam is modelled as an elastic-perfectly plastic body, of which material properties are E=206 GPa, σ_y=300 MPa, and ν=0.3. For this choice of the material properties the analytical solution for the limit bending moment for plane strain, M_{limit}, assuming the Mises yield criterion, is given by

$$M_{limit} = \frac{2}{\sqrt{3}} \sigma_y \left(\frac{h}{2}\right)^2 \tag{30}$$

where h is the thickness of the beam.

Figure 4 shows the relationship between the normalized bending moment $M/(\sigma_y h^2/4)$ and the normalized curvature χ/χ_0, where χ is the curvature corresponding to M and χ_0 is the curvature for which the outer fiber of the beam becomes plastic for the first time. It is seen that CST and 4ISO elements do not find a limit load at all; all elements across the thickness reach yield, and the moment-curvature curve continues to rise. The result of using 4 CST element yields the correct normalized load, $2/\sqrt{3}$. Finally, the present CDT element also finds the accurate result: the averaged incompressibility is a necessary and sufficient condition for a limit load.

Table 1 lists the comparison of the computational time among the four different types of finite element at χ/χ_0=12.5. The CPU time for CDT is faster than that for 4 CST by a factor of 2.5 for both of the computers used: a mainframe of HITAC-M682H or a 16-bit personal computer of NEC PC9801LX with a numerical coprocessor.

Table 1 Comparison of computational time for pure bending

	HITAC-M682H	NEC-PC9801LX
Constant strain triangle (CST)	0.268 s	67.8 s
Constant dilatation triangles (CDT)	0.577	118.3
Crossed triangles (4CST)	1.364	337.3
4-node isoparametric (4ISO)	0.389	82.8

4.2 Necking of an Elastic-Plastic Bar in Plane Strain

The necking of a rectangular bar with an initial imperfection at its central portion, is analyzed numerically for various types of finite elements: CST, 4 CST and CDT. The bar consists of an elastic-plastic isotropic work-hardening material, obeying a Swift's type empirical formula given by

$$\bar{\sigma} = 683.7\ (0.020 + \bar{\varepsilon}^{p})^{0.08} \quad \text{MPa} \tag{31}$$

where $\bar{\sigma}$ and $\bar{\varepsilon}^{p}$ is the equivalent true stress and plastic strain, respectively. The material properties of the bar are the same as those used in the pure bending except for Eq. (31) and $\sigma_y =$ 500 MPa. The finite element mesh and the geometry of the bar are shown in Fig. 5, where symmetry is assumed about both the x axis and the y axis. A relatively coarse uniform mesh as shown in Figs. 5 (a) and (b) are used in the analytical region, but for comparison a finer mesh shown in Fig. 5 (c) is used in the case of computation using CST and CDT elements. The initial length of the specimen is $2\ell_0$ and the initial width is $2(a_0 + \Delta a_0)$. Here, Δa_0 is an initial geometric imperfection that is specified to be of the form

$$\Delta a_0 = -\zeta a_0 \cos\left(\frac{\pi x}{\ell_0}\right) \tag{32}$$

where in the calculations carried out here the amplitude ζ is taken to be 0.01.

Computed curves of load and area reduction at the minimum section versus elongation are

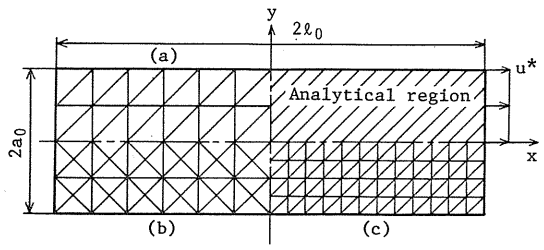

Fig. 5 Finite element systems for plane strain uniaxial tension

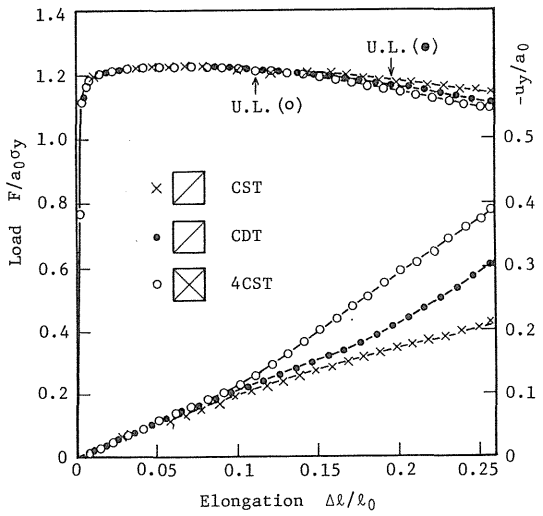

Fig. 6 Load and area reduction at the minimum section as function of elongation

shown in Fig. 6 in the case of the coarse mesh systems. There is no marked difference in the load-elongation curves in which the load reaches the maximum at around $\Delta\ell / \ell_0 = 0.08$ and then decreases monotonously. However, there are differences in the development of necking. The arrows marked U.L. in Fig. 6 denote the elongations at which unloading starts in the end parts of the model and necking starts in the center portion. Necking starts earlier for the 4 CST than the CDT elements, and develops faster and larger. On the other hand, the CST element does not show any concentration of deformation after the maximum load has been experienced.

Figure 7 shows the outer configuration of the bar and the distribution of $\bar{\varepsilon}^p$ at an elongation of $\Delta\ell / \ell_0 = 0.257$. The degrees of necking and the plastic strains confirm the results of Fig. 6. For comparison, the computed results corresponding to Figs. 6 and 7 are summarized in Fig. 8 in the

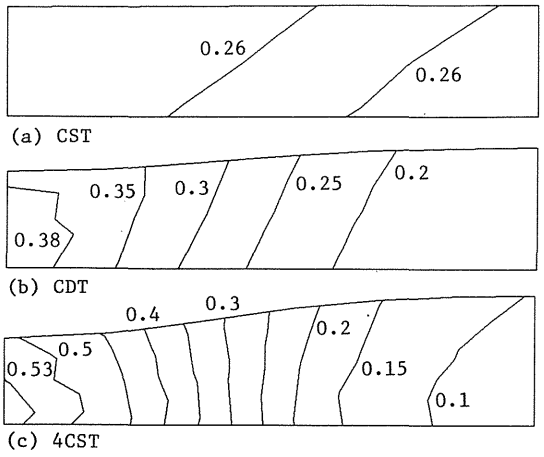

Fig. 7 Deformed shape and distribution of equivalent plastic strain at $\Delta\ell / \ell_0 = 0.257$

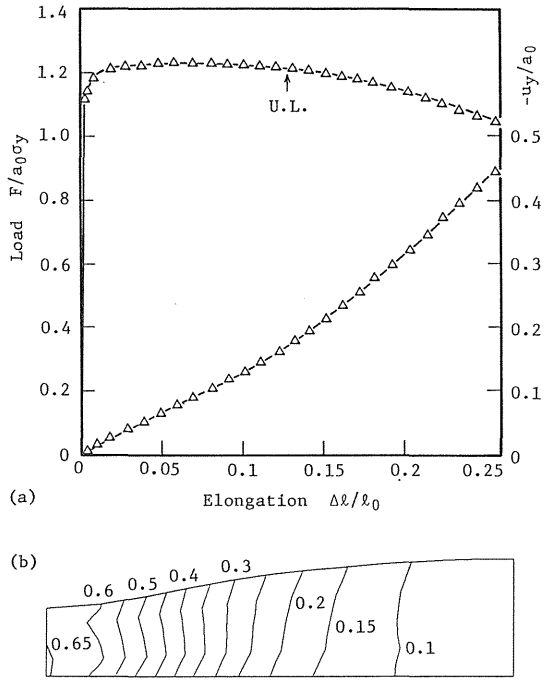

Fig. 8 Calculated results using the CDT fine mesh: (a) load and necking displacment vs. elongation curves ; (b) distribution of equivalent plastic strain at $\Delta\ell/\ell_0=0.257$

case of computation using the CDT finer mesh. It is seen that the initiation of unloading, the degree of necking and the deformation concentration become close to those for 4 CST elements. This is due to the fact that the number of total nodes, i.e. degree of freedom doubled in the finer mesh. However, the CST element yielded yet uniform deformation though the finer mesh shown in Fig. 5 (c) was used.

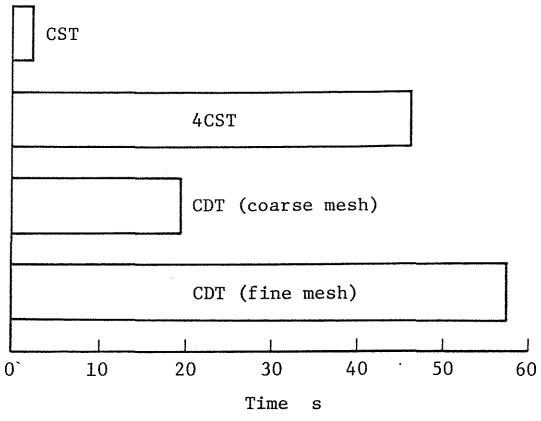

Fig. 9 Comparison of computational time for uniaxial tension

Figure 9 shows the comparison of computational time for various element types used. The CPU time of the finer CDT mesh is comparable to that of the 4 CST mesh.

5. CONCLUDING REMARKS

A finite element analysis based on updated Lagrangian formulations has been carried out to solve large deformation elastic-plastic problems involving overconstaraint phenomena due to the overstiff response of some types of finite element, particularly the widely used constant strain trianglular element (CST). Although the so-called crossed triangles (4 CST) element shown in Fig. 1 (a) has been proved to be free of overconstraint for plane strain problems [2], the 4 CST element is not so attractive from the viewpoint of computational time. Noting the efficiency, we have implemented the Nagtegaal-Rice functional using the quadrilateral element (CDT) which consists of a pair of CSTs as shown in Fig. 1 (b). If one splits the components of stress and strain into their deviatoric part and their hydrostatic part, and takes the average dilatation over the pair, the functional results in the same form as the conventional variational principle [4]. Consequently, only small changes of the velocity-strain rate matrix $[B]$ and the relevant parts make it possible to use the existing finite element computer program.

The quality of the solutions through the comparison with various element types has been examined by means of examples of pure bending and uniaxial tension. The accuracy for the CDT element is not so great as that of using the 4 CST element, but the computational time is faster by a factor of 2.5. To improve the accuracy one should trade off the efficiency by using a finer mesh.

The implementation based on the Nagtegaal-Rice functional is not restricted to a pair of triangular elements developed in this paper, but could be applied to any type and number of finite element. One of the authors [7] has formulated the functional using the eight-cornered brick element, which consists of six constant strain tetrahedra, for three-dimensional problems, and has applied it to the analysis of oblique cutting.

REFERENCES

[1] O.C.Zienkiewicz: The *Finite Element Method in Engineering Science*, 2nd ed., McGraw-Hill, London, (1971) 48.

[2] J.C.Nagtegaal, D.M.Parks and J.R.Rice: On Numerically Accurate Finite Element Solutions in the Fully Plastic Range, Comp. Meth. Appl. Mech. Eng., 4, (1974) 153.

[3] S.Nemat-Nasser and M.Taya: Numerical Studies of Void Growth in a Necked Bar, Int. J. Solids Structures, 16, (1980) 483.

[4] K.Washizu: *Variational Methods in Elasticity & Plasticity*, 3rd ed., Pergamon Press, (1983) 376.

[5] C.Truesdell: *A First Course in Rational Continuum Mechanics*, 1, Academic Press, (1977) 138.

[6] Y.Yamada: Constitutive Modelling of Inelastic Behavior and Numerical Solution of Nonlinear Problems by the Finite Element Method, Computers & Structures, 8, (1978) 533.

[7] K.Maekawa, T.Nagayama, I.Ohshima and R.Murata: Finite Element Simulation of Oblique Cutting, Bull. Japan Soc. Prec. Eng., 24, 3 (1990) 221.